



INTERNATIONAL ATOMIC ENERGY AGENCY
UNITED NATIONS EDUCATIONAL, SCIENTIFIC AND CULTURAL ORGANIZATION



INTERNATIONAL CENTRE FOR THEORETICAL PHYSICS
34100 TRIESTE (ITALY) - P.O.B. 586 - MIRAMARE - STRADA COSTIERA 11 - TELEPHONE: 2260-1
CABLE: CENTRATOM - TELEX 460392-1

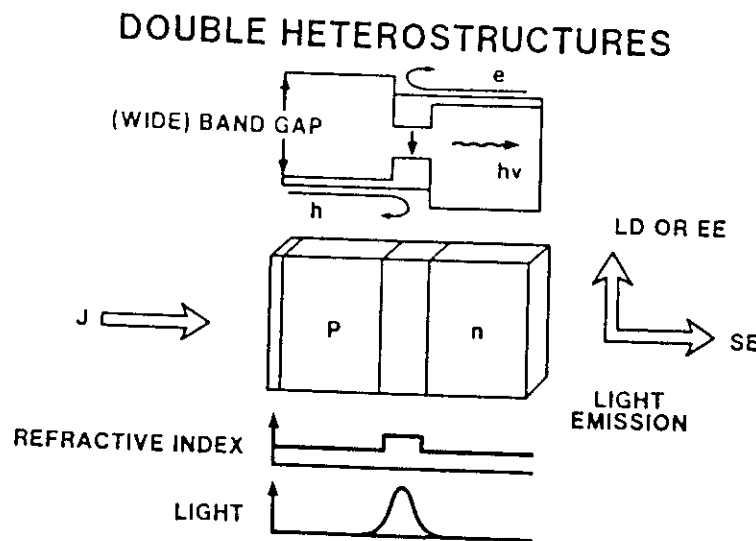
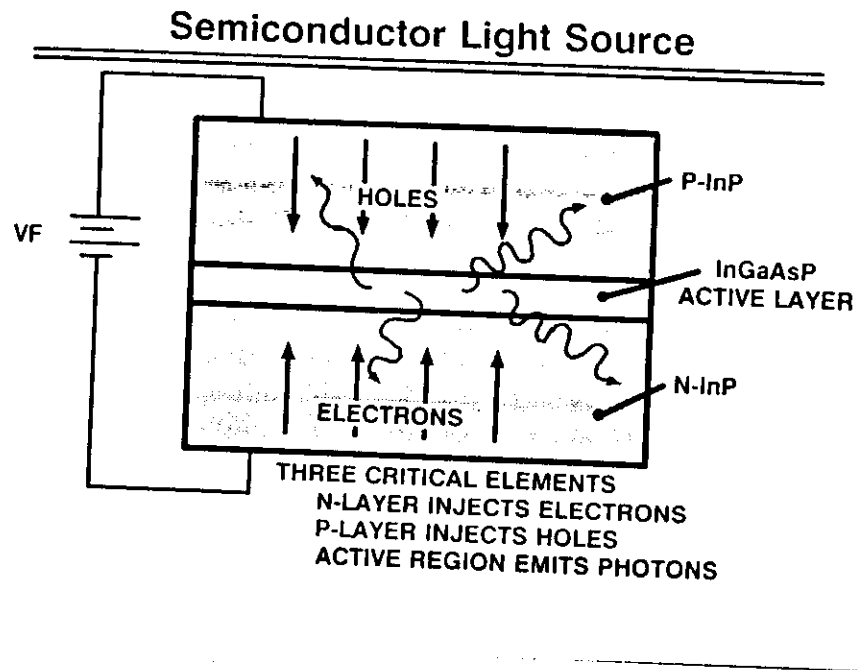
H4-SMR/285 - 12

WINTER COLLEGE ON
LASER PHYSICS: SEMICONDUCTOR LASERS
AND INTEGRATED OPTICS

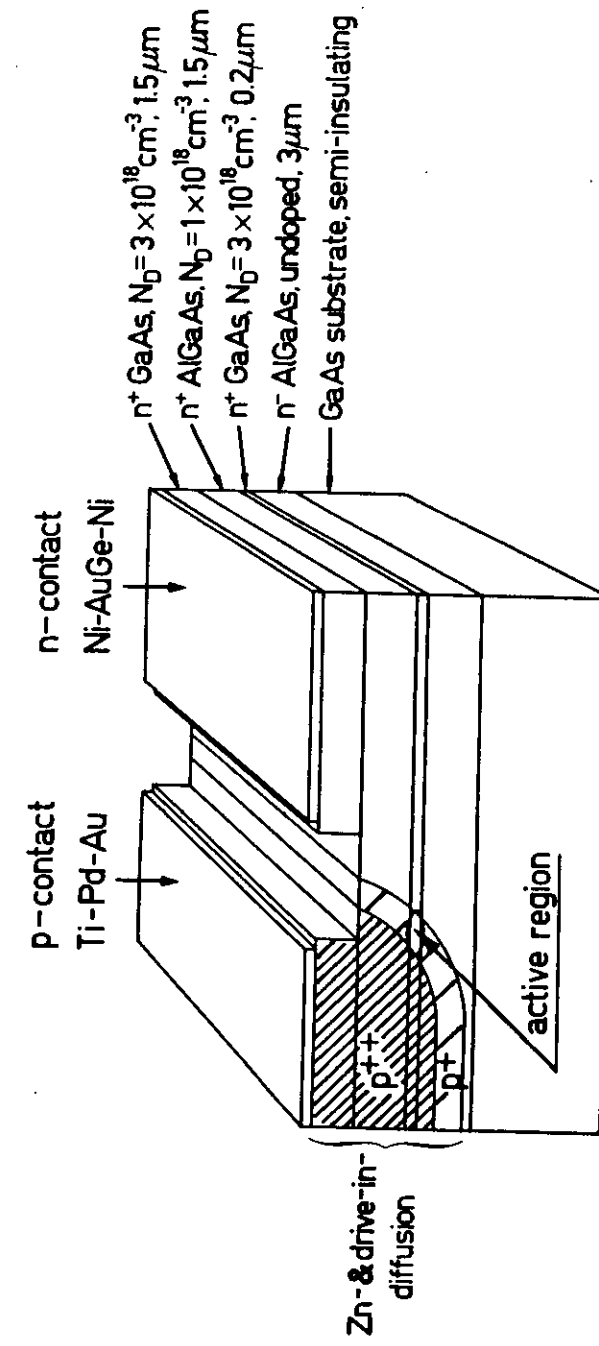
(22 February ~ 11 March 1988)

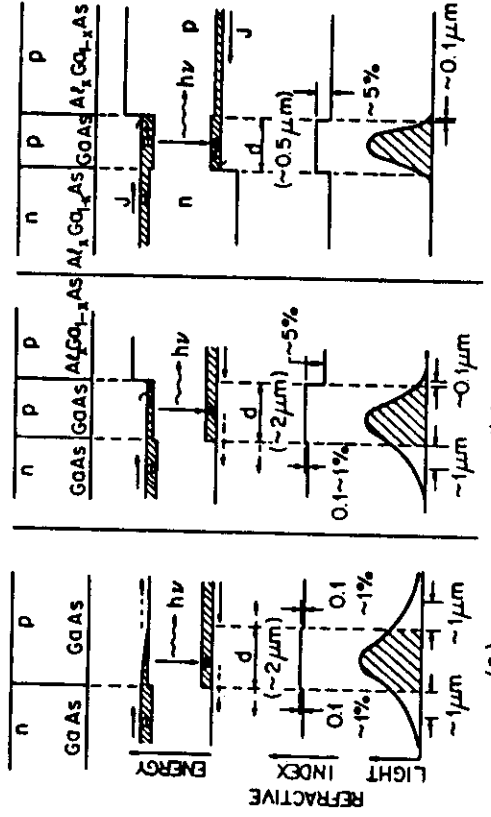
PHYSICS OF SEMICONDUCTOR
LIGHT SOURCES AND
DETECTORS

N. Melchior
Swiss Federal Institute of Technology
Zurich, Switzerland



TRANSVERSE JUNCTION STRIPE LASER





Comparison of some characteristics of (a) homostructure, (b) single-heterostructure, and (c) double-heterostructure lasers. The top row shows energy-band diagrams under forward bias. The refractive index change for GaAs/Al_xGa_{1-x}As is about 5%. The change across a homostructure is less than 1%. The confinement of light is shown in the bottom row. (After Panish, Hayashi, and Sumski.)

THRESHOLD CURRENT DENSITY

Oscillation Continuum

In the previous section, it was shown that when the excitation satisfies the necessary condition for stimulated emission, the absorption coefficient $\alpha_{\text{stim}}(E)$, which is related to $r_{\text{stim}}(E)$ by Eq. (3.2-41), becomes negative and gives $q(E)$ as

$$g(E) = -z(E) = (\hbar^3 c^4 / 8\pi\eta^2 E^2) v_{\text{sim}}(E) \quad (3.8-1)$$

The laser oscillator is usually formed by use of parallel reflecting surfaces for a medium with gain to form a Fabry-Perot etalon or interferometer.¹¹ The oscillation condition can be obtained by considering the plane wave reflection between parallel partially reflecting surfaces as shown in Fig. 11-34.

The plane wave with the complex propagation constant r' , as given by Eq. (2.2-54), is incident on the left cavity mirror as shown in Fig. 3.8-1. The cavity length is L , the ratio of transmitted to incident fields at the left mirror is taken as t_{11}' , and ratio of reflected to incident fields at the right mirror is taken as r_{11}' . The ratio of reflected to incident fields within the optical cavity is $r_1 \exp(i\beta L)$ at the left mirror and $r_2 \exp(i\beta L)$ at the right mirror.

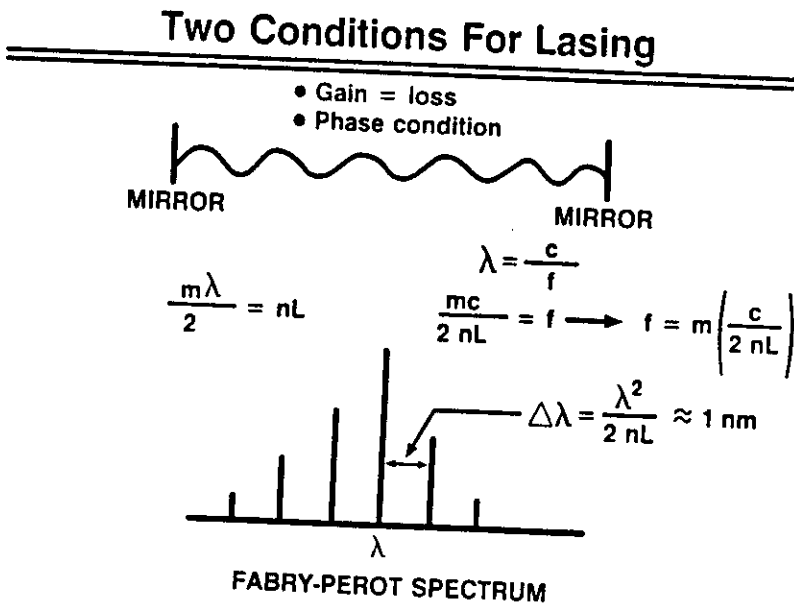


FIG. 3-6-1 Representation of the oscillation condition for a medium with gain and parallel reflectances

mirror. These complex field reflectances are related to the power reflectances $R_1 = r_1 r_1^*$ and $R_2 = r_2 r_2^*$. For a low loss medium, the phase shifts θ_1 and θ_2 are small and are generally neglected so that $r_1 = R_1^{1/2}$ and $r_2 = R_2^{1/2}$.

Without the time dependence, Eq. (2.2-46) gives the plane-wave electric field as $\delta_i \exp(-\Gamma z)$ so that δ_x is $t_1 \delta_i$ inside the left boundary and $t_1 \delta_i \exp(-\Gamma L)$ just inside the right boundary. The first portion of the field transmitted at the right boundary is $t_1 t_2 \delta_i \exp(-\Gamma L)$ and the reflected field is $t_1 t_2 \delta_i \exp(-\Gamma L)$. The next portion of the wave transmitted at the right boundary becomes $t_1 t_2 r_1 r_2 \exp(-3\Gamma L)$ and so on. Addition of these transmitted fields gives

$$\begin{aligned}\delta_i &= t_1 t_2 \delta_i \exp(-\Gamma L) [1 + r_1 r_2 \exp(-2\Gamma L) \\ &\quad + r_1^2 r_2^2 \exp(-4\Gamma L) + \dots].\end{aligned}\quad (3.8-2)$$

The sum is a geometric progression which permits Eq. (3.8-2) to be written as

$$\delta_i = \delta_i \left[\frac{t_1 t_2 \exp(-\Gamma L)}{1 - r_1 r_2 \exp(-2\Gamma L)} \right]. \quad (3.8-3)$$

When the denominator of Eq. (3.8-3) goes to zero, the condition of a finite transmitted wave δ_i with zero δ_i is obtained, which is the condition for oscillation. Therefore the oscillation condition is reached when

$$r_1 r_2 \exp(-2\Gamma L) = 1. \quad (3.8-4)$$

From Section 2.2,

$$\Gamma = j(\bar{n} - j\bar{k})k_0 \quad (2.2-54)$$

and with $k_0 = 2\pi/\lambda_0$ from Eq. (2.2-38) and with $\bar{k} = \alpha\lambda_0/4\pi$ from Eq. (2.2-61), Eq. (3.8-4) becomes

$$r_1 r_2 \exp[(g - \alpha_i)L] \exp[-2j(2\pi\bar{n}/\lambda_0)L] = 1. \quad (3.8-5)$$

In Eq. (3.8-5), the absorption term has been written as the difference between the gain and all of the losses α_i . Losses are discussed in detail in a later portion of this section. Unless the necessary conditions for stimulated emission are met, g is also a loss term and is replaced by α of Eq. (3.8-1).

The condition for oscillation given by Eq. (3.8-5) represents a wave making a round trip of $2L$ inside the cavity to the starting plane with the same amplitude and phase, within a multiple of 2π . The amplitude requirement for oscillation is

$$r_1 r_2 \exp[(g - \alpha_i)L] = 1, \quad (3.8-6)$$

or

$$g = \alpha_i + (1/L) \ln(1/r_1 r_2). \quad (3.8-7)$$

The phase condition is

$$4\pi\bar{n}L/\lambda_0 = 2m\pi \quad (3.8-8)$$

with $m = 1, 2, 3, \dots$, and becomes

$$m(\lambda_0/\bar{n}) = 2L. \quad (3.8-9)$$

The longitudinal mode spacing may be obtained by rewriting Eq. (3.8-9) as $m\lambda_0 = 2\bar{n}L$ and differentiating to obtain

$$\lambda_0 dm + m d\lambda_0 = 2L d\bar{n}. \quad (3.8-10)$$

For adjacent modes, $dm = -1$, and Eq. (3.8-9) can be substituted for m to give

$$d\lambda_0 = \frac{\lambda_0^2}{2\bar{n}L[1 - (\lambda_0/\bar{n})(d\bar{n}/d\lambda_0)]} \quad (3.8-11)$$

for the spacing between adjacent longitudinal modes.

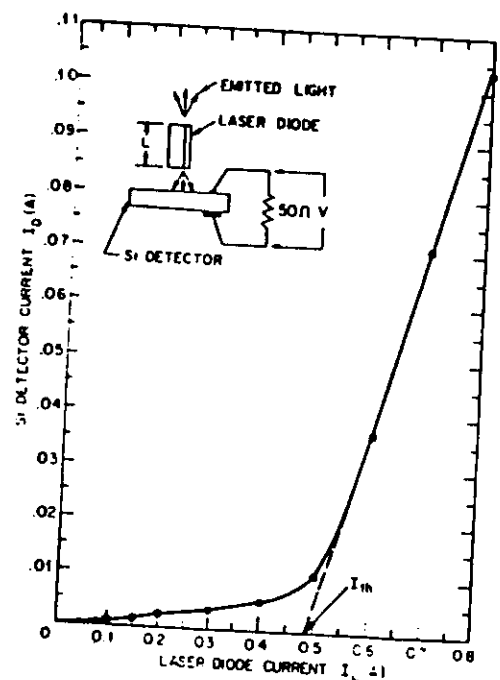
Equation (3.8-7) is generally given with the power reflectances as

$$g = \alpha_i + (1/2L) \ln(1/R_1 R_2), \quad (3.8-12)$$

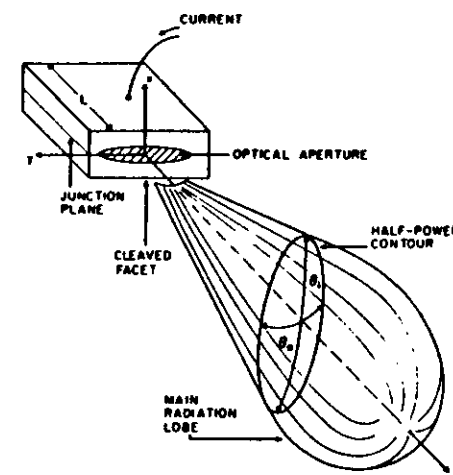
or for $R_1 = R_2 = R$, the gain requirement for laser oscillation becomes

$$g = \alpha_i + (1/L) \ln(1/R). \quad (3.8-13)$$

Laser Operating Characteristics

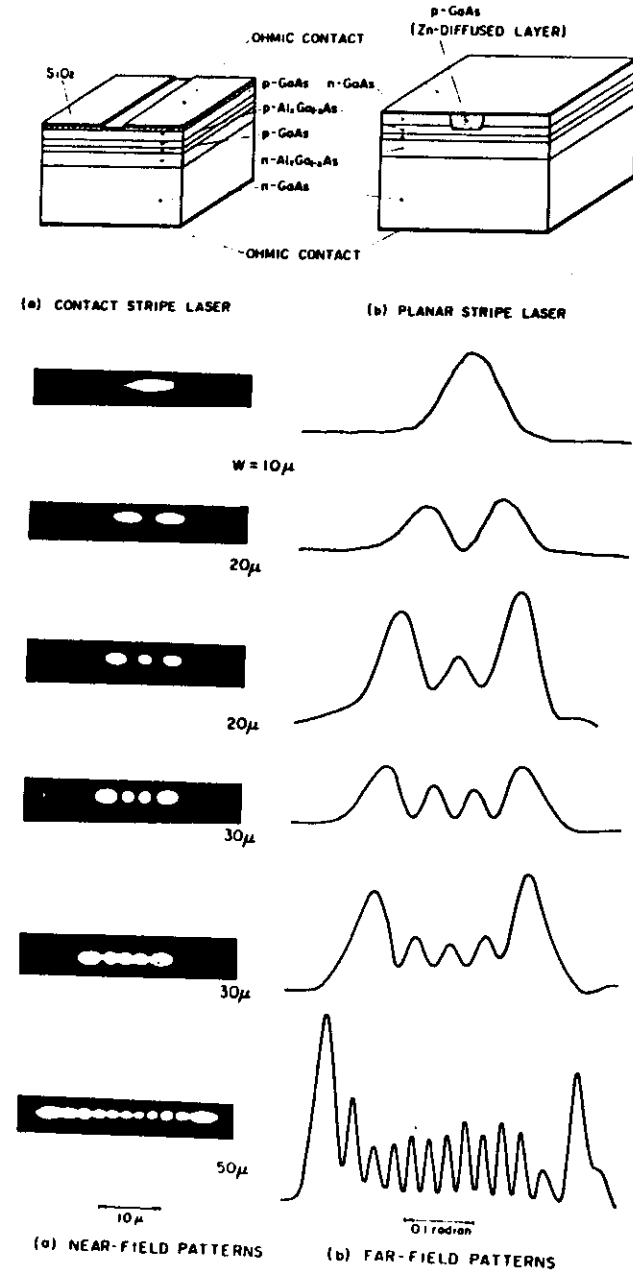


Light output versus diode current for a GaAs-Al_xGa_{1-x}As DH laser at room temperature. The insert shows the measurement setup (After Casay and Panish).

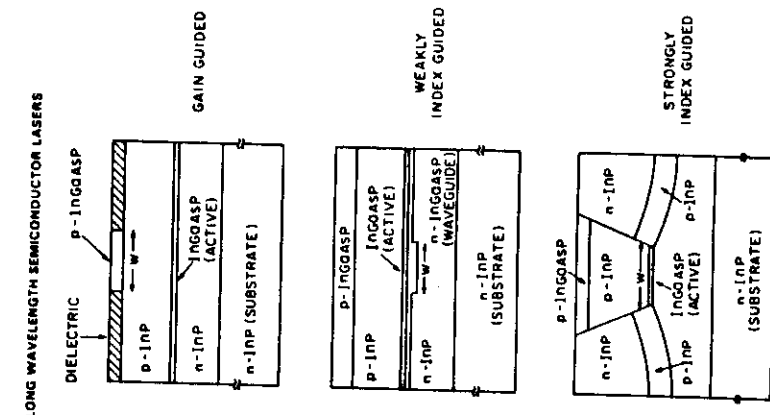


Far-field radiation patterns

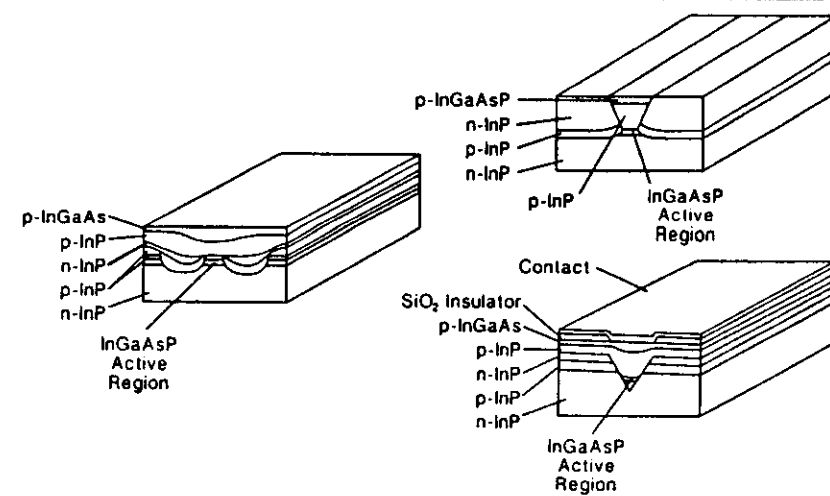
A GaAs-Al_xGa_{1-x}As Double Heterostructure Planar Stripe Laser

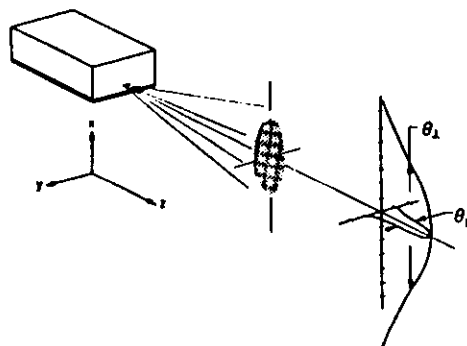
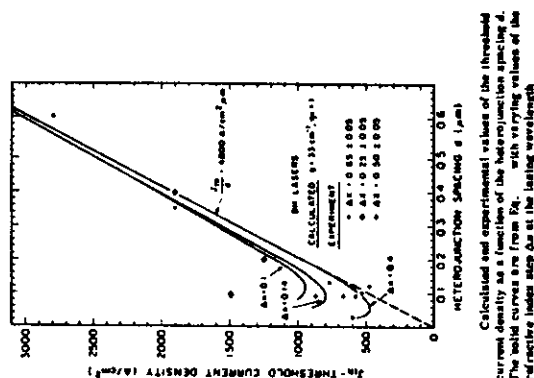


Near-field patterns (a) and far-field patterns (b) for various stripe width W values near the thresholds.



Index Guided Laser Designs





Schematic representation of far-field emission of a stripe-geometry double-heterostructure laser. The full angles at half power, perpendicular to and along the function plane, are also indicated. (After Casey and Parish).

Rate Equations of Injection Lasers

The operation of injection lasers can most easily be described in terms of time dependent rate equations for the electron and photon densities. In their simplest form, the rate equations do not contain the spatial variations of the electron and photon density distributions in the laser cavity, but treat them as suitable averages. However, photons belonging to different laser modes are treated as different variables.

The laser rate equations are nonlinear and do not have simple, exact analytical solutions.

II. LASER RATE EQUATIONS

The interchange of energy between electrons and photons in a laser is governed by spontaneous and stimulated emission processes. The rate of energy transfer between electrons and photons is described by rate equations of the form [7]

$$\frac{dn_e}{dt} = \frac{J}{cd} - \frac{n_e}{\tau_{sp}} - \frac{c}{\eta n_p} \sum_{\nu=-N/2}^{N/2} g_\nu \bar{S}_\nu \quad (1)$$

$$\frac{dS_\nu}{dt} = \frac{\gamma}{\tau_{sp}} D_\nu n_e + \frac{c}{n_p} (g_\nu - \alpha) S_\nu \quad (2)$$

with

$$g_\nu = \eta \frac{n_p}{c} A (D_\nu n_e - \hat{n}_o). \quad (3)$$

Since electron diffusion effects have been ignored, their effect on damping of relaxation oscillations is absent from this theory.

The symbols appearing in (1) through (3) are defined as follows.

η = ratio of laser volume to mode volume (mode confinement factor ≈ 0.5)

t = time coordinate

n_e = electron density in the conduction band

\hat{n}_o = a constant determining laser threshold ($2.2 \times 10^3 \mu\text{m}^{-3}$)

J = density of drive current

e = electron charge ($1.6 \times 10^{-19} \text{ C}$)

d = thickness of active laser region ($0.3 \mu\text{m}$)

D = width of laser stripe ($5 \mu\text{m}$)

τ_{sp} = spontaneous electron lifetime (typically $3 \times 10^{-9} \text{ s}$)

c = velocity of light in vacuum ($3 \times 10^{15} \mu\text{m/s}$)

n_r = refractive index of laser medium (3.4)

n_g = group index of laser medium (4)

g_ν = gain factor of ν th laser mode

S_ν = photon density of ν th laser mode

α = effective cavity loss coefficient = $\alpha_o + (1/L) \ln(1/R)$

R = reflectivity of cavity mirrors (typically 0.3)

α_o = loss coefficient ($20 \times 10^{-4} \mu\text{m}$)

γ = spontaneous emission factor (typically 3.9×10^{-1})

D_ν = line shape factor

A = stimulated emission factor (typically $1.9 \times 10^9 \mu\text{m}^3/\text{s}$)

The parameter γ accounts for the fact that only a small portion of the total spontaneous emission emitted into all directions in space contributes to the energy increase of any given laser mode. Thus, γ is the ratio of an effective element of solid angle attributable to a laser mode relative to the total solid angle 4π .

$$\gamma = \frac{\eta \lambda_p^2}{4\pi n_p^2 D d}. \quad (4)$$

The stimulated emission factor is defined as

$$A = \frac{\gamma}{\eta \tau_{sp}} D I, d/\eta. \quad (5)$$

The line shape factor D_ν is assumed to have Lorentzian shape.

$$D_\nu = \frac{\Delta \lambda_c / (\pi \Delta \lambda_D)}{1 + [(\lambda_\nu - \lambda_p)/\Delta \lambda_D]^2}. \quad (6)$$

In this formula λ_p is the wavelength at the peak of the distribution ($1.3 \mu\text{m}$), λ_ν = the wavelength of the ν th laser mode, $\Delta \lambda_D$ is the effective gain spectral linewidth parameter (typically $6 \times 10^{-2} \mu\text{m}$) [7] and

$$\Delta \lambda_c = \lambda^2 / (2 n_p L). \quad (7)$$

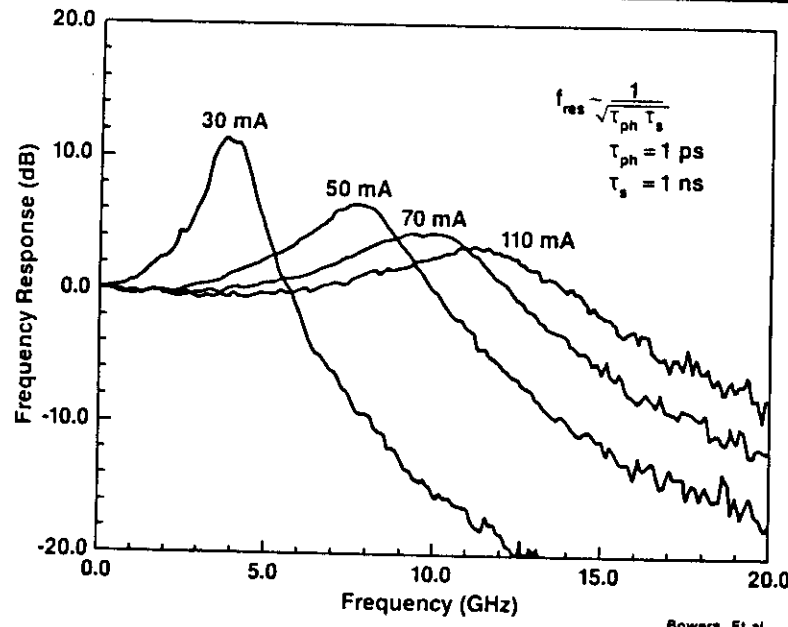
($\Delta \lambda_c$ typically $8.45 \times 10^{-4} \mu\text{m}$) is the spacing between adjacent laser modes in a cavity of length L ($250 \mu\text{m}$).

The steady-state solutions are obtained from (1) through (3) by setting the time derivatives equal to zero. Indicating steady-state quantities by an overbar we find

$$\bar{n}_e = \tau_{sp} \left[\frac{J}{cd} - \frac{c}{\eta n_p} \sum_{\nu=-N/2}^{N/2} \bar{g}_\nu \bar{S}_\nu \right] \quad (8)$$

$$\bar{S}_\nu = \frac{n_p \gamma D_\nu}{c(\alpha - \bar{g}_\nu) \tau_{sp}} \bar{n}_e. \quad (9)$$

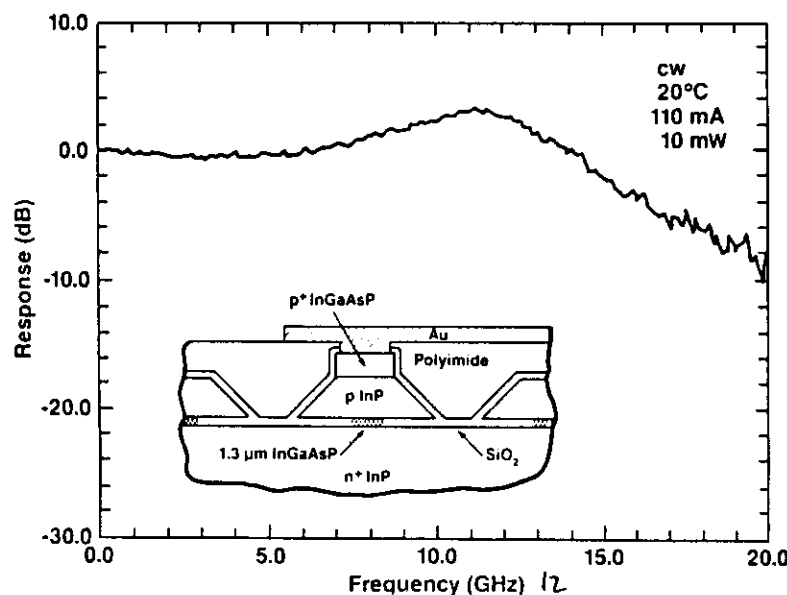
LASER MODULATION RESPONSE



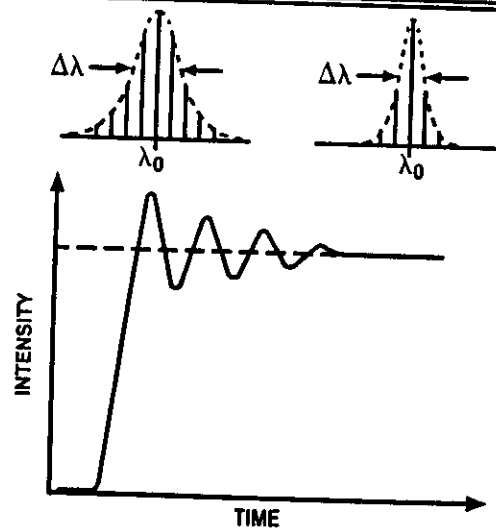
Frequency of Relaxation Oscillations

$$\omega = \left[\frac{1 + \eta A \hat{n}_o \tau_{ph}}{\tau_{sp} \tau_{ph}} \left(\frac{J}{J_{th}} - 1 \right) \right]^{1/2}$$

HIGH SPEED CONSTRICTED MESA LASERS



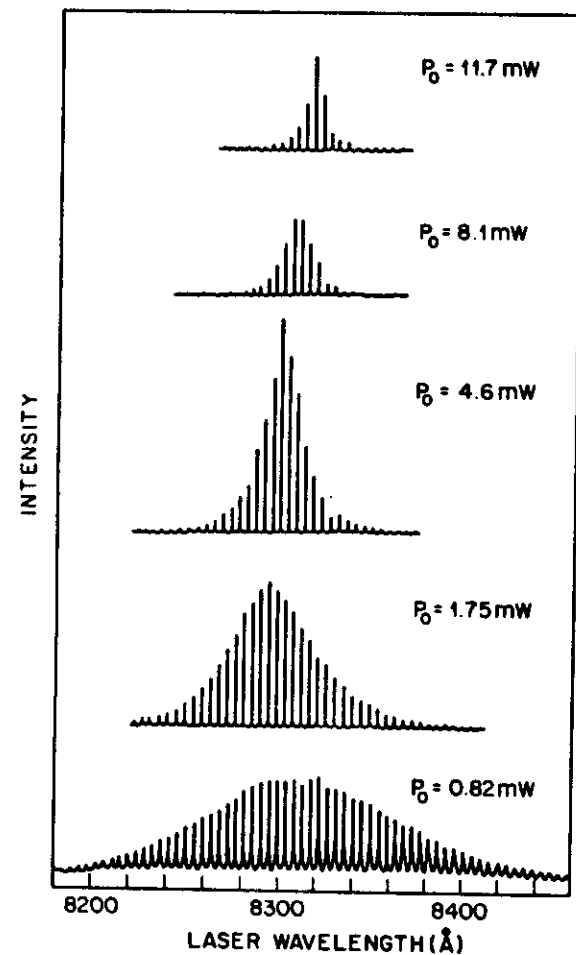
Transient Spectra Of A Multi-Mode Laser



Consequences:

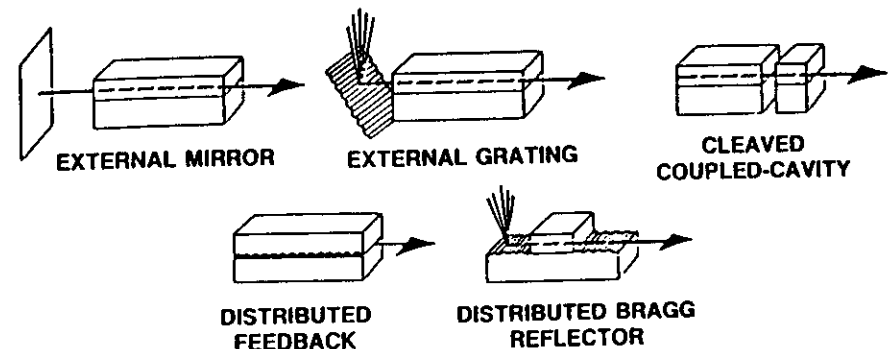
- Broadening of spectral width at high bit-rate
- Dispersion limit
- Mode partition noise

Longitudinal-Mode Spectrum

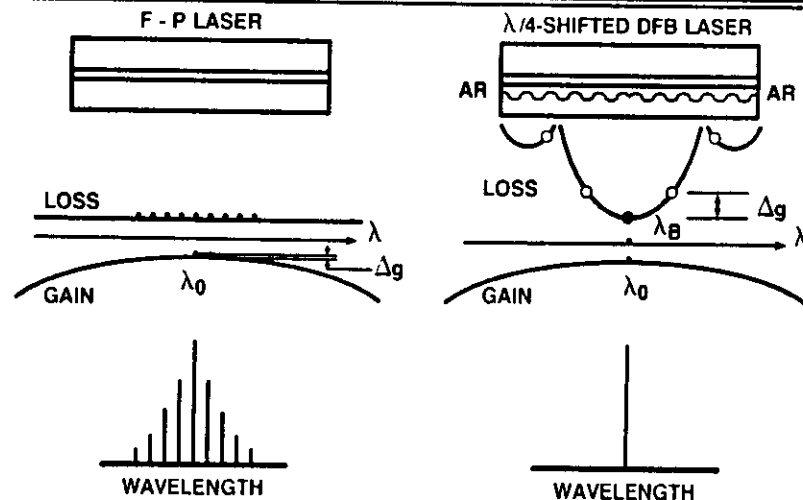


Longitudinal-mode spectra of a gain-guided laser observed at several power
Experimental spectra for an index-guided laser

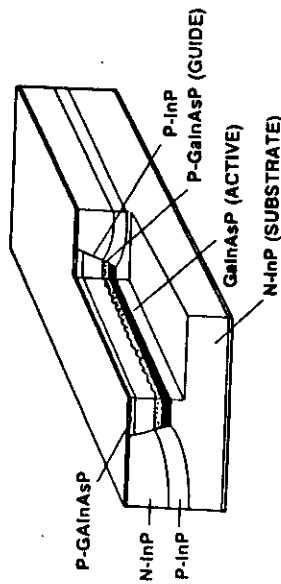
SINGLE LONGITUDINAL MODE LASERS



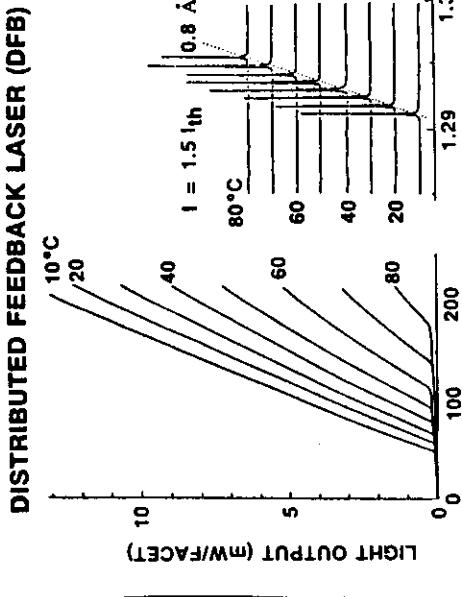
Single Frequency Operation Of DFB Lasers



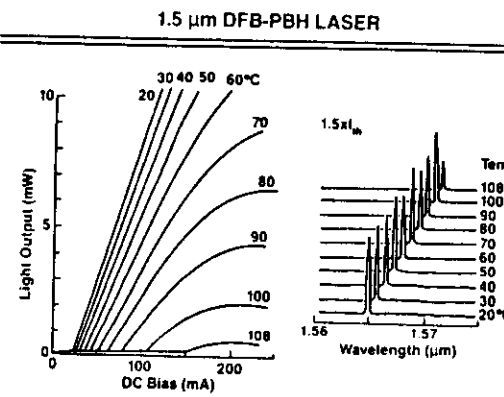
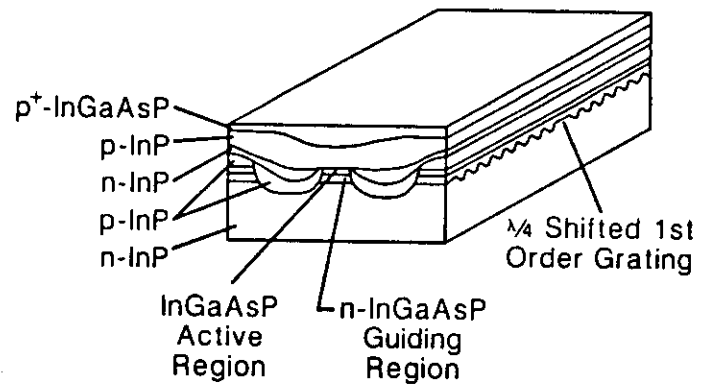
DISTRIBUTED FEEDBACK BURIED HETEROSTRUCTURE LASER DFB-BH



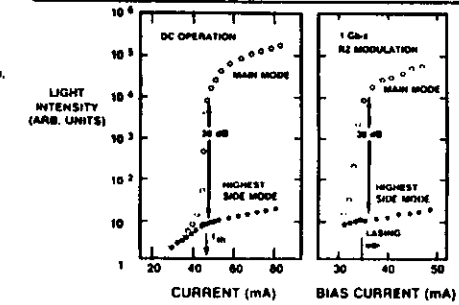
- Formation of grating
- Match grating and gain peak
- Three steps of crystal growth
- $\lambda/4$ - phase shifted grating



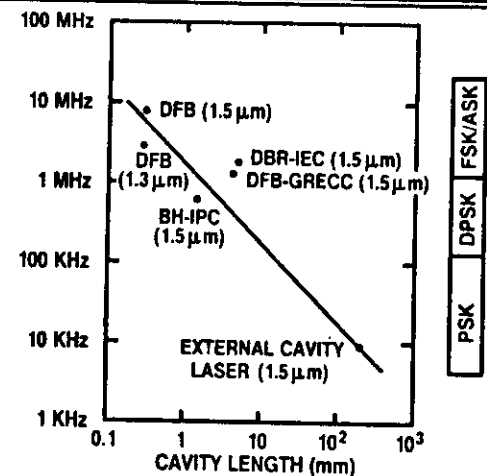
DOUBLE-CHANNEL PLANAR BURIED HETEROSTRUCTURE DFB LASER



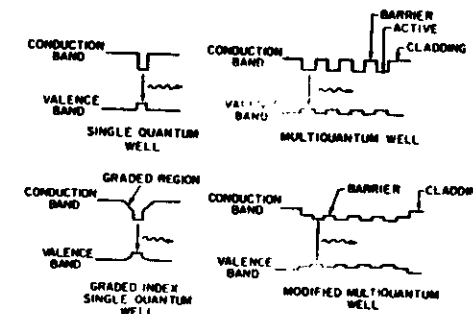
Characteristics Of An AR-Coated DFB Laser



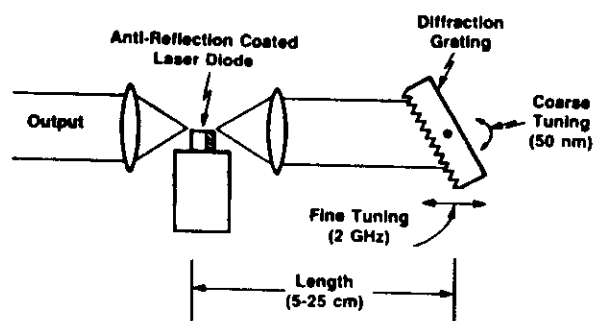
Minimum Linewidth Of Various Types Of Semiconductor Lasers



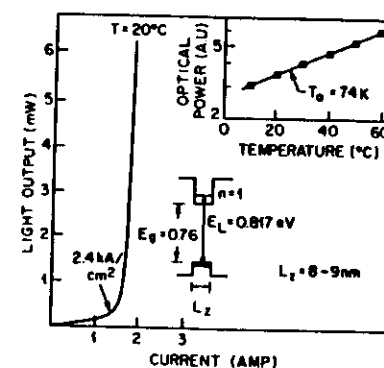
QUANTUM-WELL SEMICONDUCTOR LASERS



External Grating Laser



QUANTUM-WELL SEMICONDUCTOR LASERS



Optical Detectors

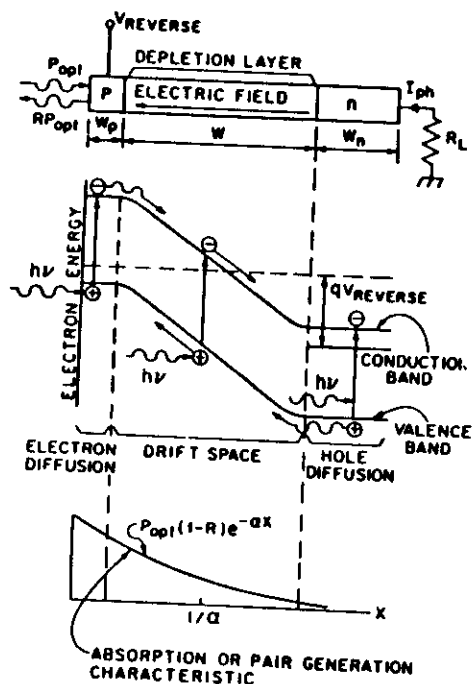
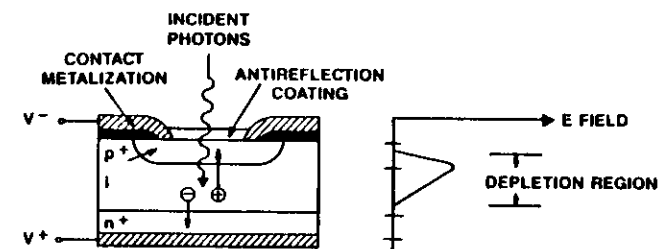
- Basic Requirements

- Sensitive at Desired Wavelength
- High Quantum Efficiency (Photon to Electron Conversion Efficiency)
- Fast Response Time (High Bandwidth)
- Low Noise

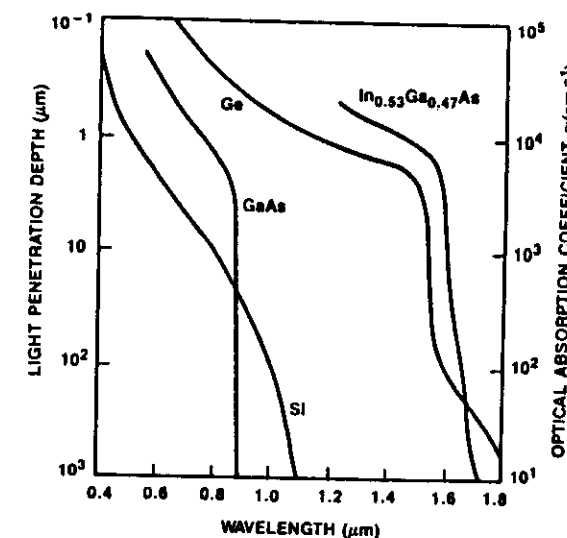
- Devices

- PIN Photodiode
- Avalanche Photodiode

PIN Photodiode



Optical Absorption Coefficient and Light Penetration Depth



Photodiode Detection Efficiency

- Quantum Efficiency η

$$\eta = \frac{\text{Number of Photoelectrons}}{\text{Number of Incident Photons}}$$

$$= (1 - r) \cdot (e^{-\alpha_1 d}) \cdot (1 - e^{-\alpha W})$$

Reflection Loss Absorption Loss Absorption Efficiency

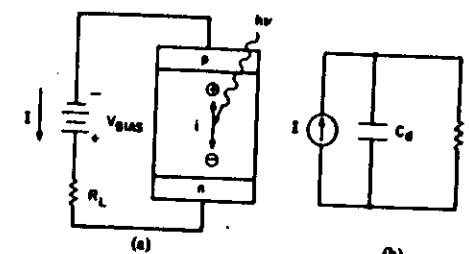
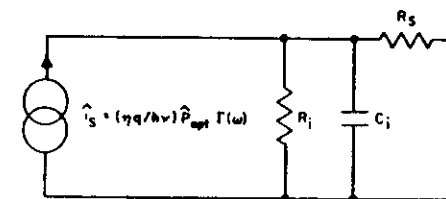
- Responsivity R (Amps/Watt)

$$R = \frac{\text{Detected Photocurrent}}{\text{Incident Optical Power}}$$

$$= \eta \frac{q\lambda}{hc}$$

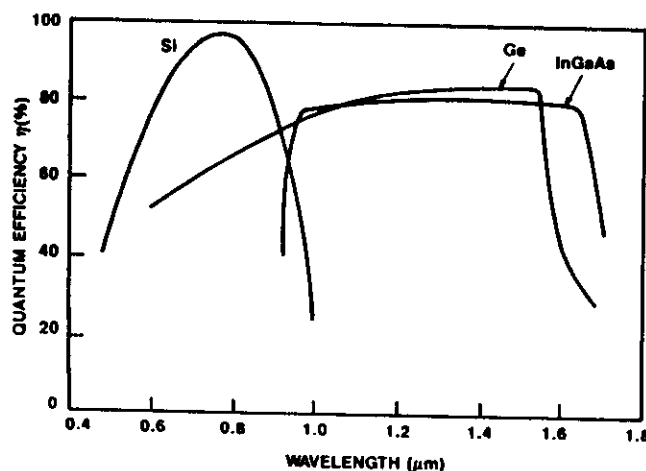
Ideal Case: $\eta = 100\%$

$$R = \begin{cases} 0.684 \text{ A/W at } \lambda = 0.85 \mu\text{m} \\ 1.046 \text{ A/W at } \lambda = 1.3 \mu\text{m} \\ 1.248 \text{ A/W at } \lambda = 1.55 \mu\text{m} \end{cases}$$



(a) Schematic representation of a p-i-n photodiode. (b) Equivalent circuit.

Typical Photodiode Spectral Response



PHOTODIODE

Photoresponse:

$$I_{ph} = ne \frac{P_{opt}}{h\nu}$$

P_{opt} = Optical Power

I_{ph} = Photocurrent

n = Quantum Efficiency

$h\nu$ = Photon Energy

e = Electronic charge

Photodiode Noise:

$$\frac{\langle I_{ph}^2 \rangle}{\Delta f} = 2e I_{ph}$$

(Spectral Noise $\langle I_{ph}^2 \rangle$ per unit Bandwidth Δf)

Response Time of PIN Photodiodes

Response Time is Limited by:

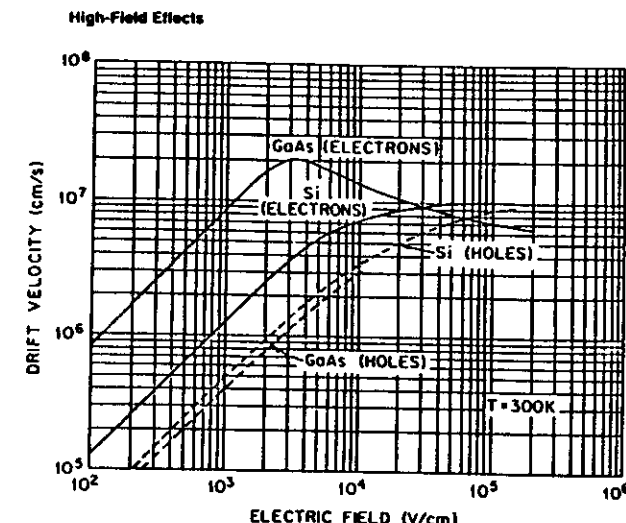
1. Carrier Transit Time

- Maintain Adequate Field in i Region so that Carriers Travel at Saturation Velocity — Very Low Doping Level
- Reduce Width of Depletion Layer for Fast Response
- However, Want Wide Depletion Layer for High Quantum Efficiency and Low Capacitance

2. RC Time Constant (Detector Capacitance and Output Load)

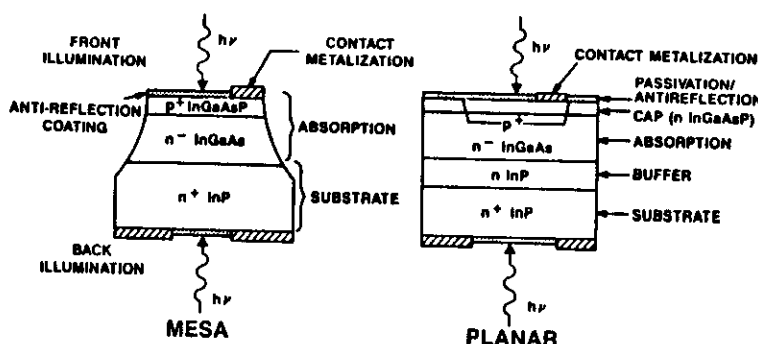
- Low Doping of i Region Reduces C
- Minimize Device Area to Reduce C (Also Reduces Dark Current)

3. Diffusion of Carriers Generated Outside of Depletion Region



Drift velocity versus electric field in GaAs and Si. Note that for n-type GaAs, there is a region of negative differential mobility.

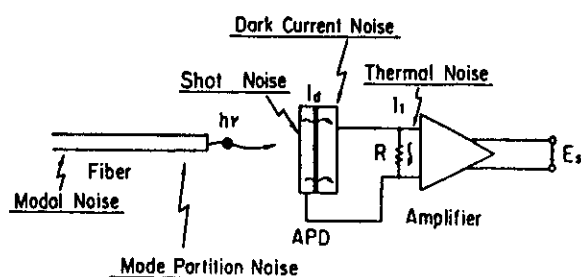
InGaAs PIN Photodiodes



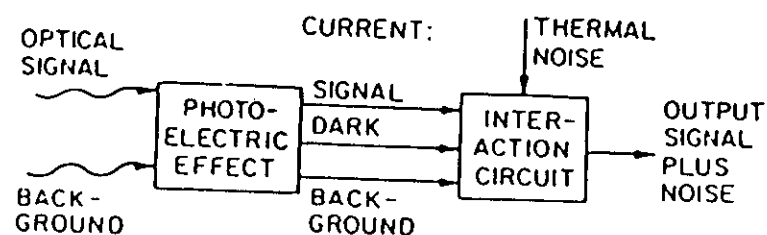
Photodiode Dark Current

- Detector Dark Current is a Source of Shot Noise and Must be Minimized for High Receiver Sensitivity, Especially at Low Bit Rates
- Generally Depends in Some Exponential Fashion on Temperature and on Material Bandgap, so is Most Serious at High Temperatures and in Long Wavelength Detectors
- Sources of Dark Current:
 1. Generation - Recombination Current in Depletion Region
 $I_{g-r} \propto \exp[-E_g/2kT]$
 2. Diffusion of Thermally Generated Minority Carriers into Depletion Region from Surrounding Undepleted Regions
 3. Surface Leakage - Reduced by Passivation
 4. p-n Junction Defects
 5. Tunnelling - Important for High Fields (e.g., APD's) and in Low Bandgap Materials. Reduced in InGaAs APD's by having Multiplication Region in InP.

NOISE IN OPTICAL RECEIVER



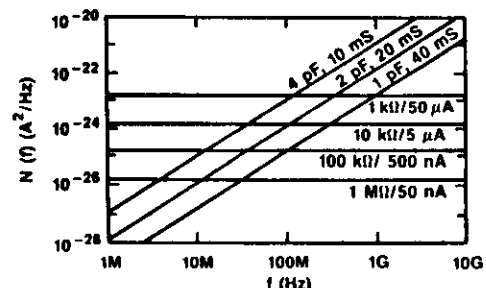
Signal-to-Noise Ratio



Noise Spectrum of FET Front End

$$N(f) = \frac{4kT}{R_L}$$

- Thermal Noise of Load or Feedback Resistor
- + $2q I_{gate}$
- Shot Noise of FET Gate Leakage Current
- + $\frac{4kT\Gamma}{g_m} (2\pi C_T)^2 f^2$
- Thermal Noise of FET Channel



ANALOG TRANSMISSION

$$\text{SNR} = \frac{E_1, \text{ Signal Power}}{E_1, \text{ Noise Power}} \quad \text{at input of receiver}$$

$$\text{SNR} = \frac{1/2(m \tau_{ph})^2}{\int \left(\frac{\langle i_{\text{Ampl}} \rangle^2}{B} + \frac{\langle i_{\text{Det}} \rangle^2}{df} \right) df}$$

m = Modulation Depth

B = Bandwidth $\approx 1/2$ Bitrate (B_r)

$\langle i_{\text{Ampl}} \rangle^2$ = Amplifier Noise

FET-Amplifier:

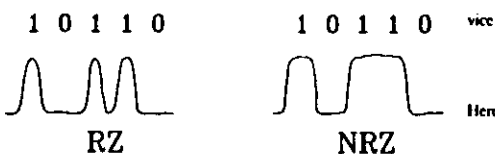
$$\frac{\langle i_{\text{Ampl}} \rangle^2}{B} df \approx 4kT \frac{0.7}{g_m} (2\pi \cdot EC)^2 \frac{B_r^3}{24}$$

g_m = Transconductance of FET

EC = Capacitance of Detector, Amplifier-input and Mount

DIGITAL TRANSMISSION

Digital Receiver Sensitivity

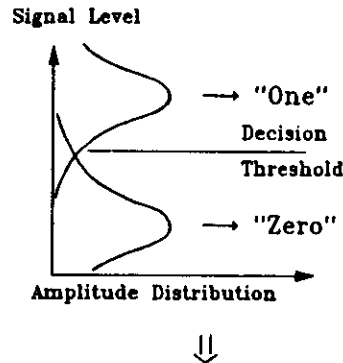


The probability of mistakenly identifying a mark as a space (or vice versa) during the detection interval is called the bit-error rate, given by:

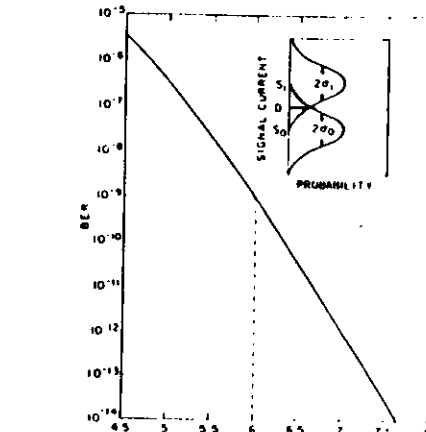
$$BER = \frac{1}{\sqrt{2}\pi} \int_0^{\infty} \exp\left(-\frac{x^2}{2}\right) dx = \frac{1}{2} \operatorname{erfc}\left(\frac{Q}{\sqrt{2}}\right).$$

Here,

$$Q = (D - s_{0,1})/\sigma_{0,1},$$

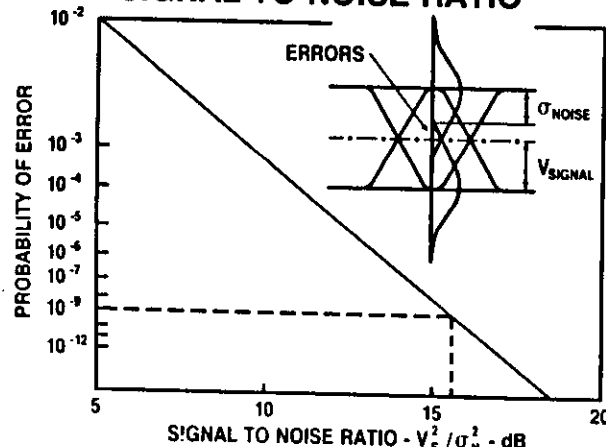


Error Rate (Complementary Error Function of Signal Power)

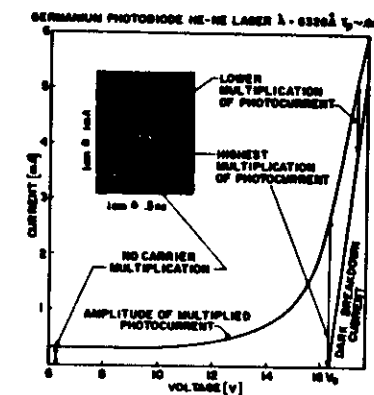


Bit-error rate versus Q . Inset: Signal current i corresponding to a mark and a space indicating the variance σ and decision level D . A Gaussian probability distribution is assumed. The shaded area in the tails of the distributions overlapping D indicates the probability for selecting an error.

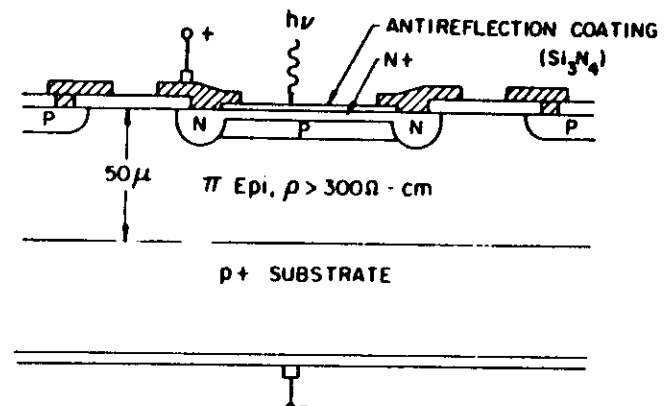
LIGHTWAVE SYSTEM PERFORMANCE MEASURES SIGNAL TO NOISE RATIO



AVALANCHE PHOTODIODE

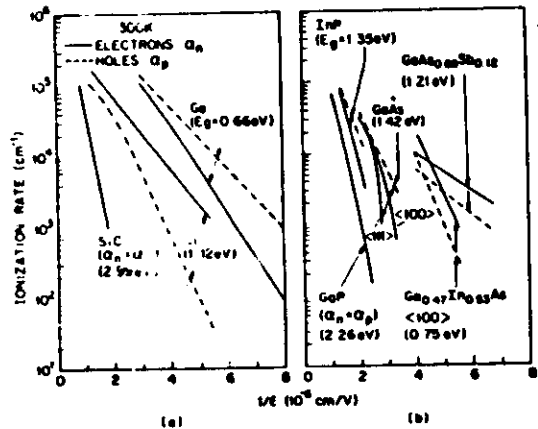
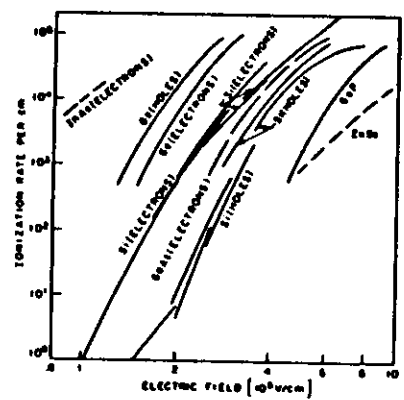


SILICON n^+ - p - π - p^+ AVALANCHE PHOTODIODE

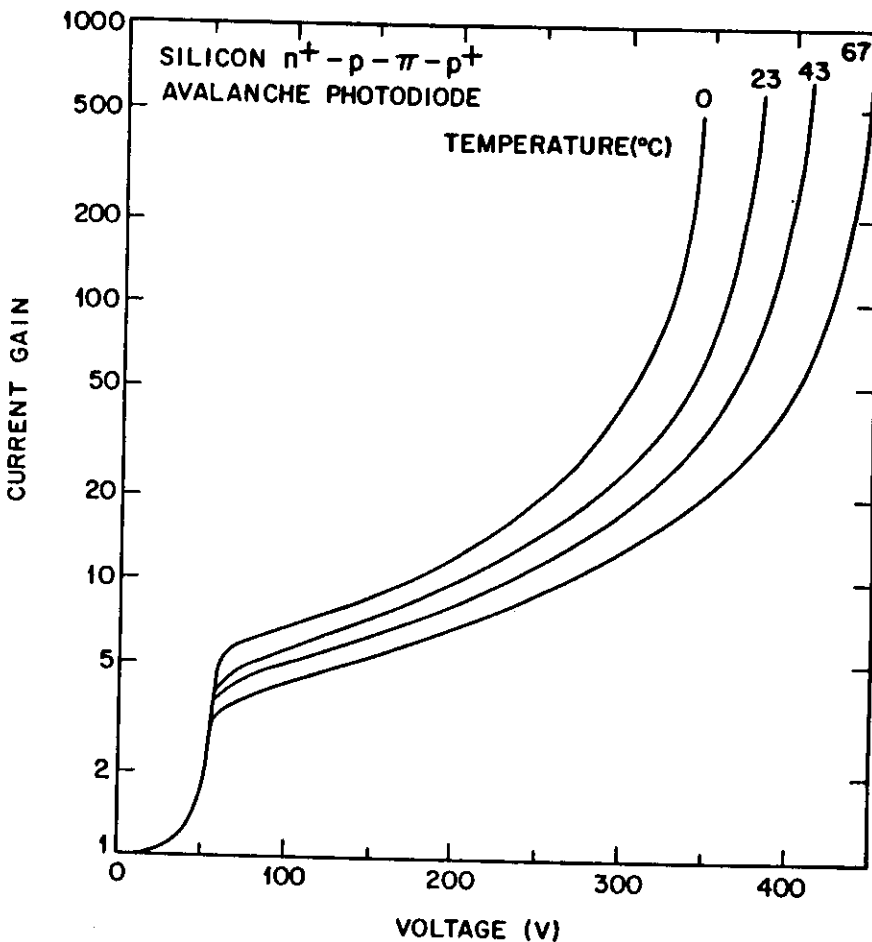


multiplication factor given by

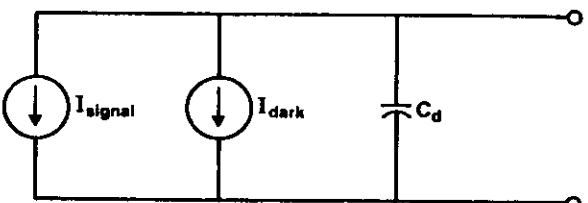
$$M(x) = \frac{\exp\{-\int_0^x (\alpha - \beta) dx'\}}{1 - \int_0^x \alpha \exp\{-\int_0^{x'} (\alpha - \beta) dx''\} dx}$$



Ionization rates at 300 K versus reciprocal electric field for Ge, Si, GaAs, and some IV-IV and III-V compound semiconductors. (After Logan and Sze, Ref. 63, Grant, Ref. 64, Glover, Ref. 65, Pearsall et al., Ref. 66, Umebu, Choudhury, and Robeson, Ref. 67, Logan and White, Ref. 68, Pearsall, Ref. 69, Pearsall, Nahory, and Pollack, Ref. 70.)



Photodiode Equivalent Circuit



$$I_{\text{signal}} = RGP$$

$$I_{\text{dark}} = I_{du} + GI_{dm}$$

where R = Responsivity (Amps/Watt)

G = Avalanche Gain ($G=1$ for PIN)

P = Incident Optical Power

I_{du} = Unmultiplied Dark Current

I_{dm} = Primary Multiplied Dark Current

NOISE IN AVALANCHE PHOTODIODES

AVALANCHE PHOTODIODE (with internal current gain M)

AVALANCHE CARRIER MULTIPLICATION IS A STATISTICAL PROCESS WHICH INCREASES THE FLUCTUATIONS OF THE PHOTODETECTION PROCESS

- POISSON'S STATISTIC IS ALTERED

- SHOT NOISE INCREASES

$$\overline{i^2} = 2 q I_{ph} M^2 F(M) \Delta f$$

$F(M)$ = NOISE FACTOR OF AVALANCHE GAIN PROCESS

multiplied photocurrent:

$$I = I_{ph} \cdot M$$

Noise spectral density:

$$\frac{\langle i^2 \rangle}{\Delta f} = 2eI_{ph} \cdot M^2 \cdot F(M)$$

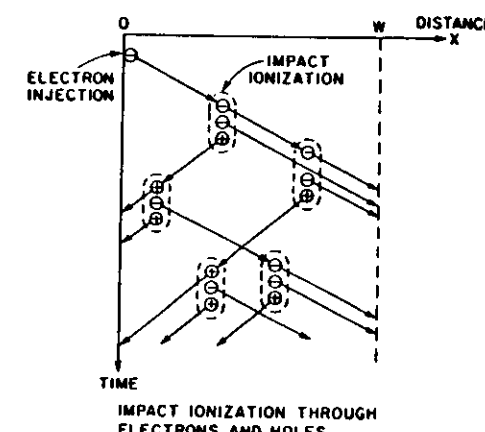
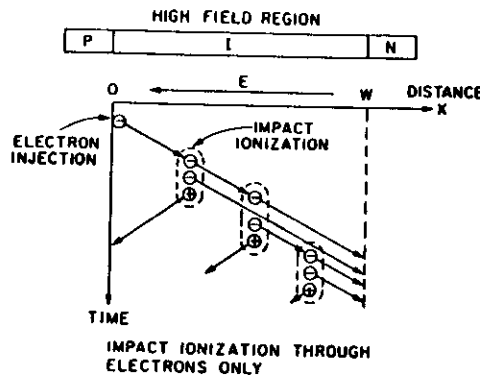
$F(M)$ = Excess Noise Factor

After Mc Intyre:

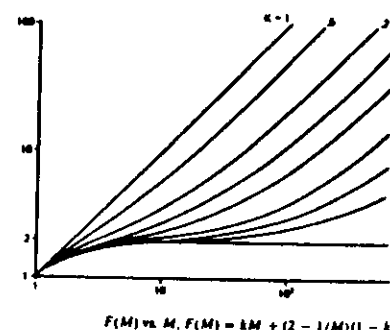
$$F(M) = kM + (2 - \frac{1}{M}) (1-k)$$

(for avalanche initiated with strongly ionizing carriers)

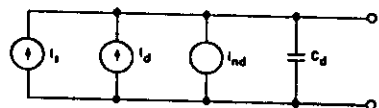
k = ratio of smallest to largest ionization coefficient for holes and electrons



Excess Noise Factor of APD



Photodiode Equivalent Circuit



- SIGNAL CURRENT

$$I_s = RGP$$

- DARK CURRENT

$$I_d = I_{du} + GI_{dm}$$

- NOISE CURRENT

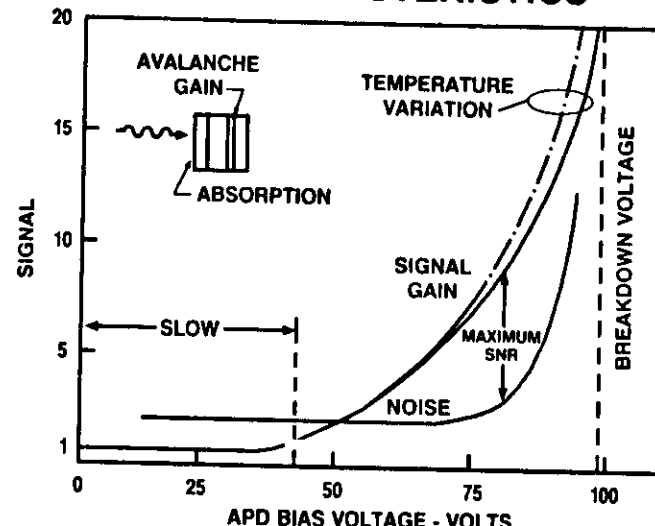
$$\langle I_{nd}^2 \rangle = 2\alpha I_{du} B_w + 2\alpha I_{dm} G^2 F(G) B_w$$

WHERE $F(G)$ IS AVALANCHE EXCESS NOISE FACTOR

$$F(G) = kG + (1-k)(2-1/G)$$

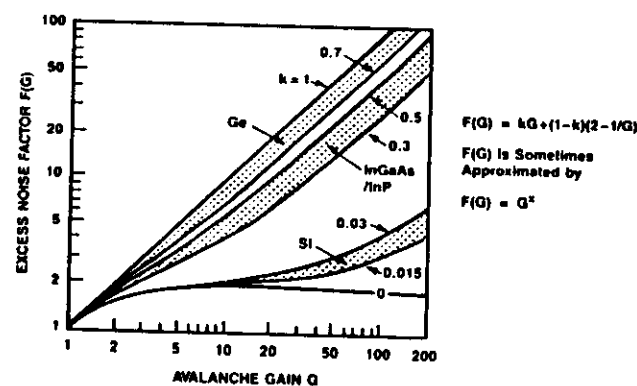
k IS RATIO OF IONIZATION CONSTANT OF HOLES AND ELECTRONS OF APDS

APD CHARACTERISTICS



APD Excess Noise Factor

Excess Noise Factor $F(G)$ Depends Upon the Ratio k of Impact Ionization Probabilities for Electrons and Holes in the Semiconductor Material where Avalanche Gain Occurs

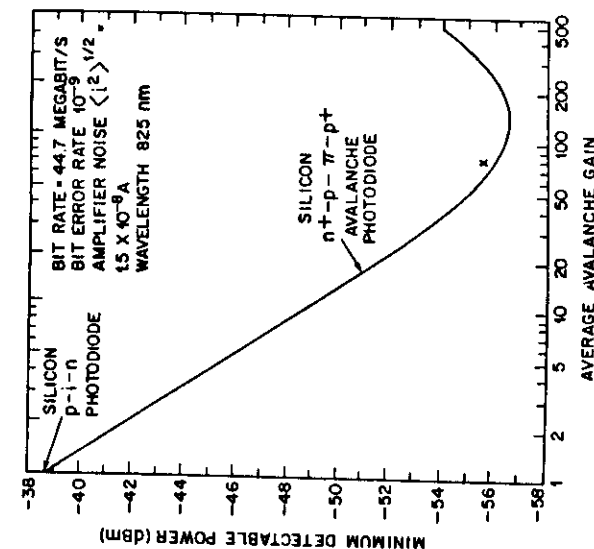
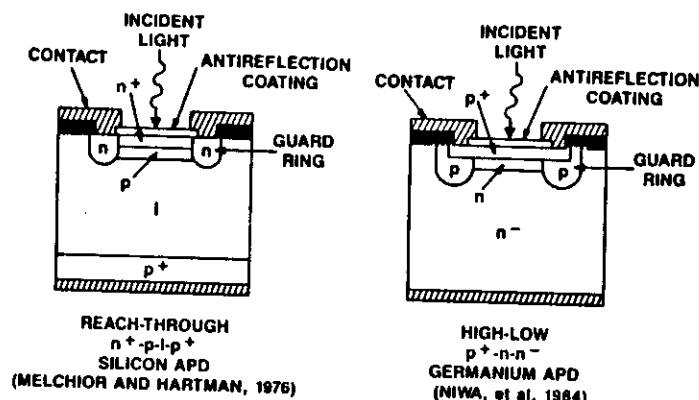


Response Time of Avalanche Photodiodes

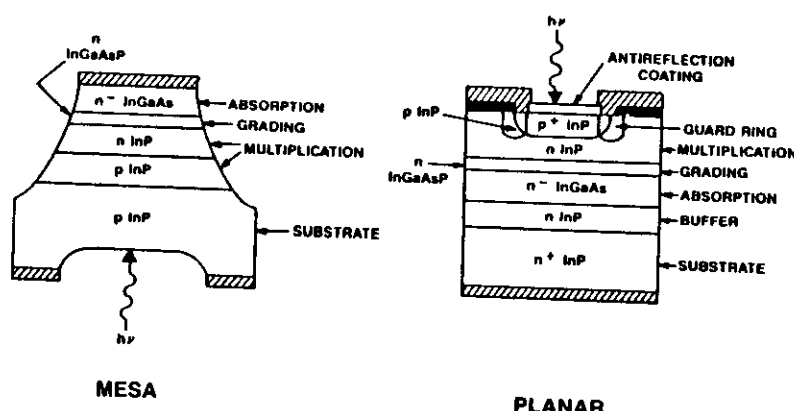
APD Response Time is Limited by:

1. Carrier Transit Time
 - More Layers Required than for PIN Photodiode
 2. Avalanche Build-up Time (at High Gain)
 - Depends Upon Thickness of Multiplication Region and on Ratio k of Electron and Hole Ionization Coefficients. Low k — Both Low Noise and High Speed
 3. RC Time Constant
 4. Hole Trapping at InGaAs/InP Heterojunction Interface
 - Speed Improved by Using InGaAsP Grading Layers Between Absorption and Multiplication Regions
- At Low Gain, Transit Time and RC Effect Dominate
 - Constant Bandwidth
 - At High Gain, Avalanche Build-up Time Dominates. Bandwidth Decreases Proportionately with Increasing Gain
 - Constant Gain-Bandwidth Product

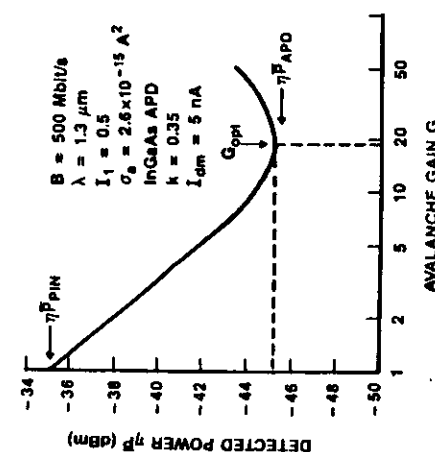
Silicon and Germanium Avalanche Photodiodes



Separate Absorption, Grading, and Multiplication (SAGM) InGaAs APD



APD Receiver Sensitivity



Receiver Sensitivity

PIN Detector:

$$\bar{\eta P} = \frac{hc}{q\lambda} Q \sigma_a$$

where $Q = \text{Signal/Noise Ratio}$
 $= 6$ for 10^{-9} BER

APD Detector (neglecting dark current):

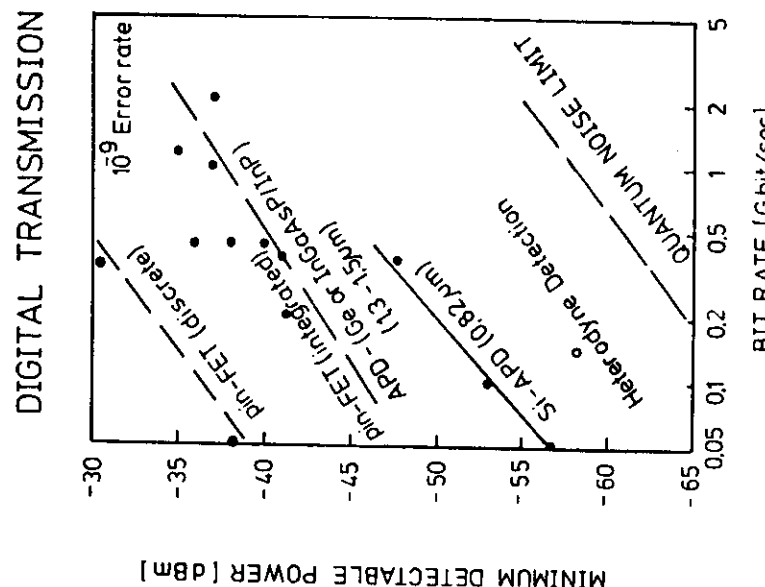
$$\bar{\eta P} = \frac{hc}{q\lambda} Q \left[\frac{\sigma_a}{G} + q B I_1 Q F(G) \right]$$

$$G_{\text{opt}} = \left(\frac{\sigma_a}{kq B I_1 Q} \right)^{1/2}$$

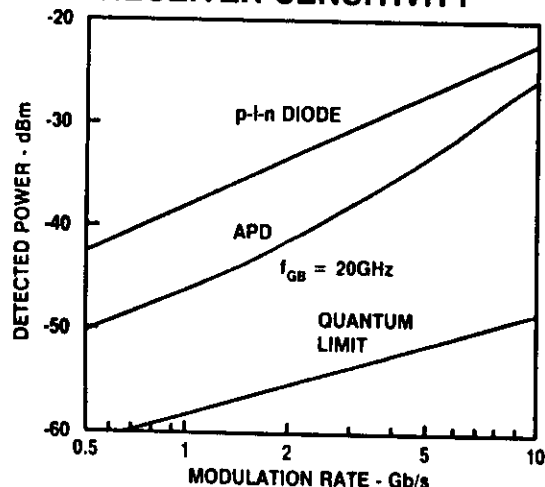
$$\bar{\eta P}_{\text{APD}} = \left(\frac{2}{G_{\text{opt}}} \right) \bar{\eta P}_{\text{PIN}}$$

Typical Improvement Over PIN:

Si APD	14-17 dB
Ge APD	5-8 dB
InGaAs APD	7-10 dB



LIGHTWAVE SYSTEMS RECEIVER SENSITIVITY



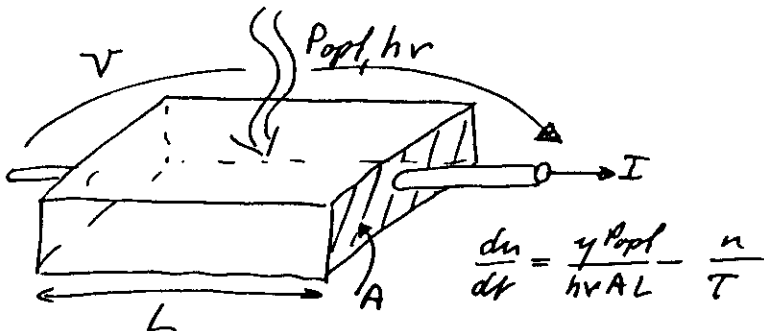
Photodiode Characteristics

	InGaAs PIN	Ge APD	InGaAs APD	Si APD
Quantum Efficiency	η	0.8 (0.95)	0.8 (0.9)	0.8 (0.95)
Bandwidth (GHz)	f_{GB}	5 (>60)	1 (3)	3 (8)
Capacitance (pF)	C_d	0.5 (0.05)	0.5 (0.2)	0.5 (0.1)
Dark Current (nA)	I_{du}	10 (<0.1)	100 (50)	10 (2)
Dark Current (nA)	I_{dm}		100 (5)	10 (2)
Ionization Ratio	k		1.0 (0.7)	0.4 (0.3)
Gain-Bandwidth Product (GHz)			10 (20)	20 (70)

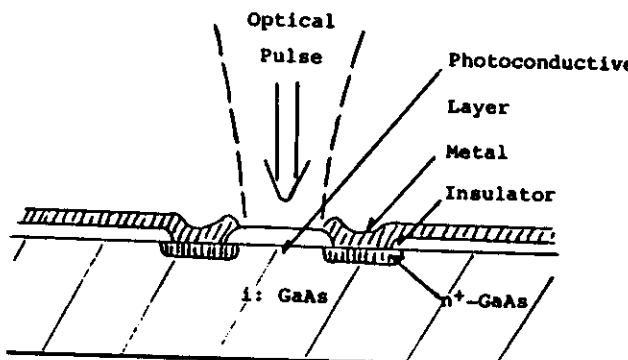
Notes:

1. Typical (Best)
2. Best Parameters may not be Achievable Simultaneously In the Same Device.

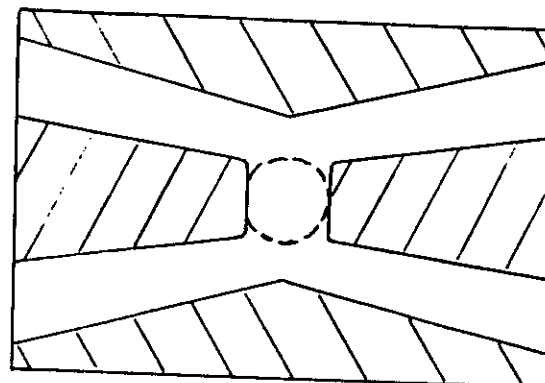
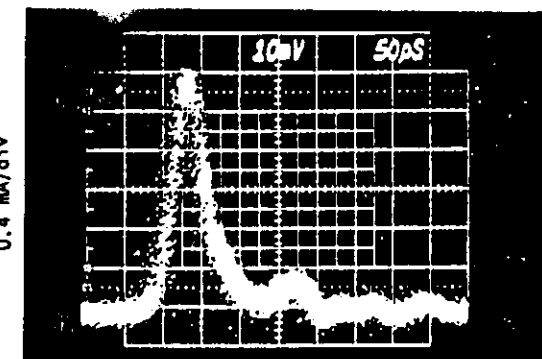
IDEAL PHOTOCOCONDUCTOR



HIGH-SPEED PHOTOCODUCTIVE SWITCH

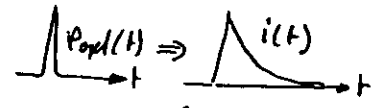


Planar Photoconductor



Broadband Microwave Mount :
Tapered Coplanar Waveguide

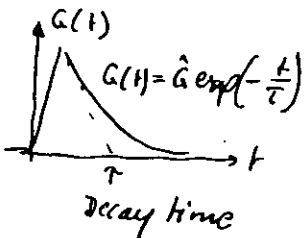
SS



$$\alpha n = \alpha p = \frac{\gamma P_{opt} dt}{hv AL}$$

$$\hat{I} = e(\mu_n + \mu_p) \frac{\gamma \int P_{opt} dt}{hv} \frac{V}{L^2}$$

$$\Delta \hat{G} = e(\mu_n + \mu_p) \frac{\gamma (P_{opt} dt)}{hv} \frac{1}{L^2}$$



$$\frac{\Delta n}{T} = \frac{\gamma P_{opt}}{hv AL}$$

$$\Delta n \propto \Delta p$$

hole current.

$$I = \epsilon \mu_p T \frac{\gamma P_{opt}}{hv} \frac{V}{L^2}$$

$$G = \epsilon \mu_p T \frac{\gamma P_{opt}}{hv} \frac{1}{L^2}$$